Three-dimensional Modelling of Poorly Detailed RC Frame Joints

R. Eligehausen, J. Ožbolt, G. Genesio, M. S. Hoehler

Institute of Construction Materials, University of Stuttgart, Germany

S. Pampanin

Department of Civil Engineering, University of Canterbury, Christchurch, New Zealand.

2006 NZSEE Conference

ABSTRACT: This paper presents preliminary work on three-dimensional numerical modelling of seismic strengthening measures for poorly detailed reinforced concrete frames, primarily designed for gravity loads, as was typical in seismic-prone countries before the introduction of more advanced seismic codes in the early 1970s. These buildings are at risk due to inadequate structural detailing, deficiencies in reinforcement anchorage and the absence of measures to prevent brittle failure modes. Representative beam-column joints tested experimentally at the University of Pavia are analyzed using a continuum finite element program specially developed for detailed modelling of fracture in quasi-brittle materials. The microplane material model with relaxed kinematic constraint is used for the concrete. In the first stage of this work, which is presented in this paper, the proper modelling of the behaviour of smooth reinforcement with hooked ends, as well as the accurate representation of brittle shear failure modes in joints, are of particular interest. In the second stage of the project, strengthening measures that incorporate post-installed anchors for connection to the existing structure will be assessed.

Keywords: *Beam-column joints, Existing RC frames, Plain round bars, Hook anchorage, Finite elements, Microplane model.*

1 INTRODUCTION

The goal of the present work is to model strengthening measures for reinforced concrete (RC) frames designed for gravity loads only in order to improve their performance under seismic load. The origin of the problem stems from design rules in use prior to the early-mid 1970s, thus before the introduction of adequate seismic code provisions along with capacity design principles/

Most buildings designed and constructed before the 1970s lack ductility in joint regions due to inadequate reinforcement detailing (lack of transverse reinforcement), poor bond properties of the reinforcement (plain round or smooth bars) and deficiencies in the anchorage details (hooked end bars, insufficient lap splices). These factors can cause brittle failure. A particular "concrete wedge" brittle failure mechanism due to the interaction of shear cracking and stress concentration at the hook anchorage location was observed by Pampanin et al. (2002) in cyclic tests on exterior beam-column T-joint subassemblies carried out at the University of Pavia.

In this paper these experimental results are reviewed and compared with numerical analyses performed using the finite element code MASA, developed at the University of Stuttgart and capable of three-dimensional (3D) nonlinear analysis of concrete, concrete-like materials and reinforced concrete structures. The program is based on the microplane model with relaxed kinematic constraint (Ožbolt et al. 2001). It has been shown that the code is able to realistically predict the behaviour of reinforced concrete structures (Ožbolt et al. 1998).

In future research, strengthening measures that incorporate post-installed anchors for connection to the existing structure will be investigated using the numerical models developed in this paper.

Following a brief description of the investigated test specimens, the microplane constitutive law for concrete and the employed finite element model are described. The results of the numerical analysis are then compared with the experimental results. Additionally, a parameter study was carried out to investigate the influence of several parameters including the stiffness of the reinforcement hook, the constitutive bond law, the strength of the bond and the local bending stiffness of reinforcement bars on the response of the beam-column subassembly under monotonic lateral loading. Finally, the influence of the relevant parameters on the reversed cyclic behaviour of the connection is discussed.

2 TEST SPECIMEN

The specimen that was modelled was selected from a series of experimental tests on two-thirds scale, beam-column subassemblies performed at the University of Pavia (Pampanin et al. 2002). The complete test series was comprised of two exterior knee-joints, two exterior T joints and two interior (cruciform) joints. Exterior T-joint T1 was selected for modelling. The details of the T-joint are shown in Figure 1.
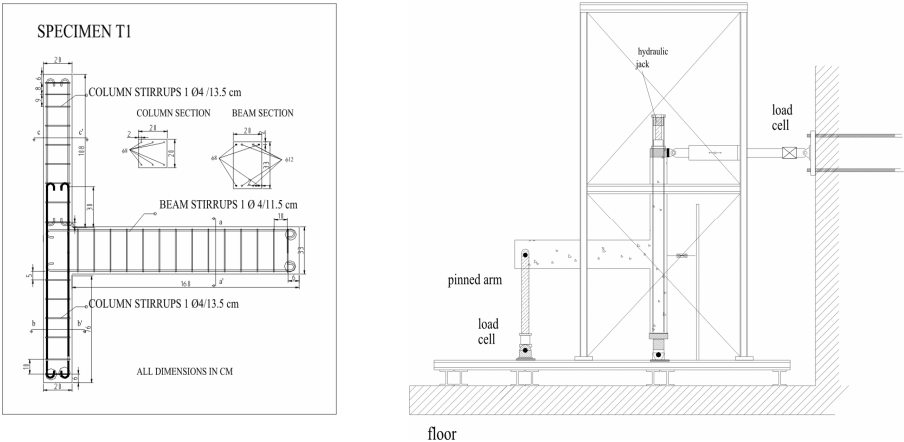

Figure 1. Exterior beam-column joint specimen T1 and test set-up (Pampanin et al. 2002).

The test specimen was loaded under reversed cyclic loading. The imposed loading history consisted of a series of three cycles at increasing top drift levels of ±0.2, ±0.6, ±1.0, ±1.5, ±2.0, ±3.0 and ±3.5 percent (Figure 2a). To reproduce the asymmetric effects during an actual cyclic push-pull test on the prototype frame system, the axial load in the column was varied during the experiments as a function of the lateral load (N = 100 kN – 2.44F where F = lateral force; Figure 2b).

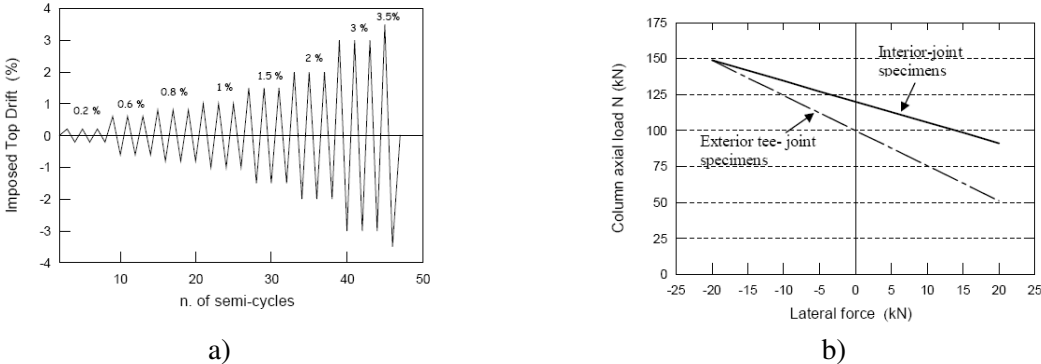a)   b)

Figure 2. Load history: a) subassembly drift; b) axial vs. lateral load relation (Pampanin et al. 2002)

3 FINITE ELEMENT MODEL

The goal of the first part of the present numerical study was to investigate the influence of various parameters on the response of the beam-column connection. In the used finite element (FE) code, a microplane material model for concrete and a trilinear steel constitutive law for reinforcement were used. The bond between steel and concrete was simulated using discrete bond elements.

2

3.1 Microplane model

The microplane model is a three-dimensional, macroscopic model in which the material is characterized by uniaxial relations between the stress and strain components on planes of various orientations called "microplanes". At each finite element integration point the microplanes can be imagined to represent damage planes or weak planes of the microstructure of the material. The macroscopic response is obtained by integrating contributions of all microplanes. More details can be found in Ožbolt et al. (2001).

3.2 Bond model

The correct simulation of the bond between concrete and reinforcement bars plays a central role in the proper modelling of beam-column connections. When the bond forces tend to zero it is evident that the majority of the shear force will be transferred across the joint core by a diagonal compression strut mechanism and hence severe diagonal tension cracking is less likely if bond deterioration occurs at an early stage of loading (Park 2002). A complex interaction between flexural response of the adjacent beam element and the joint shear transfer mechanism occurs also due to the stress penetration into the panel zone from the beam bars, combined with a fixed-end rotation in the beam due to progressive bond degradation and pull out mechanism.

The discrete bond model implemented in MASA consists of a one-dimensional (1D) finite element (Figure 3) with a realistic bond-slip relationship (Figure 4). Additional information on the discrete bond model can be found in Ožbolt et al. (2002) or Lettow (2006).
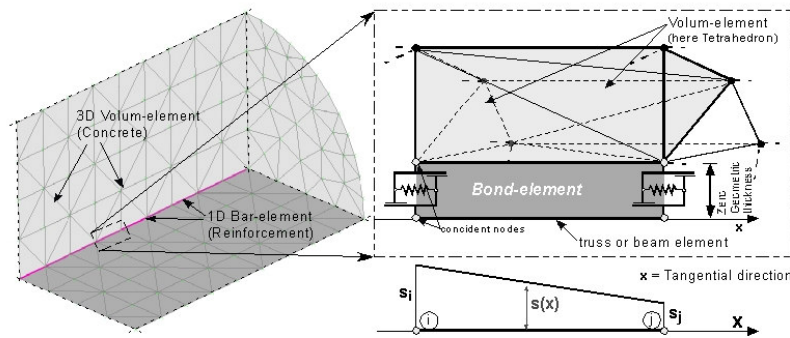

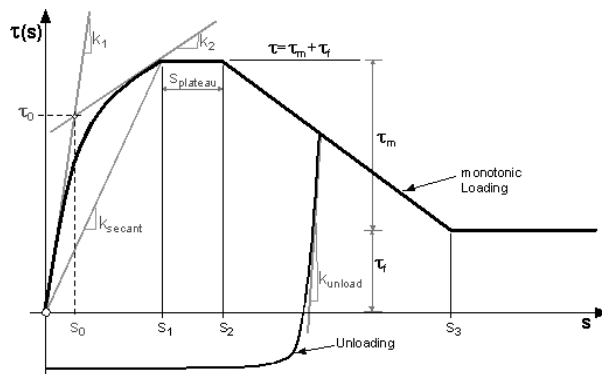Figure 3. Basic assumptions of the bond model implemented in MASA (Lettow 2006).

Figure 4. Bond-slip relationship for deformed bars (Lettow 2006).

It has been demonstrated that the model is able to correctly predict bond behaviour of deformed steel bars for monotonic and cyclic loading (Eligehausen et al. 1983; Ožbolt et al. 2002).

The calibration of the parameters defining the bond elements has been carried out referring to the results of beam tests on straight plain round bars performed by Fabbrocino et al. (2002). For bars with a diameter of 12 mm the total bond strength was approximately $\tau_m + \tau_f = 1$ MPa (τ_m = mechanical bond; τ_f = frictional bond) for a slip of $s_1 = 0.03$ mm. During cycling, the bond degradation valid for deformed bars is principally due to the shear failure of concrete between the ribs of the bar. In the case

of smooth bars, as adopted in the test specimens, it is reasonable to assume that friction is the only source of bond mechanism at the steel-concrete interface and that it is scarcely influenced by the cycling. Figure 5 shows the stress-slip behaviour of the discrete bond model for monotonic and cyclic loading, including the general assumption for deformed bars (Figure 5a) and the calibrated parameters for smooth bars (Figure 5b).
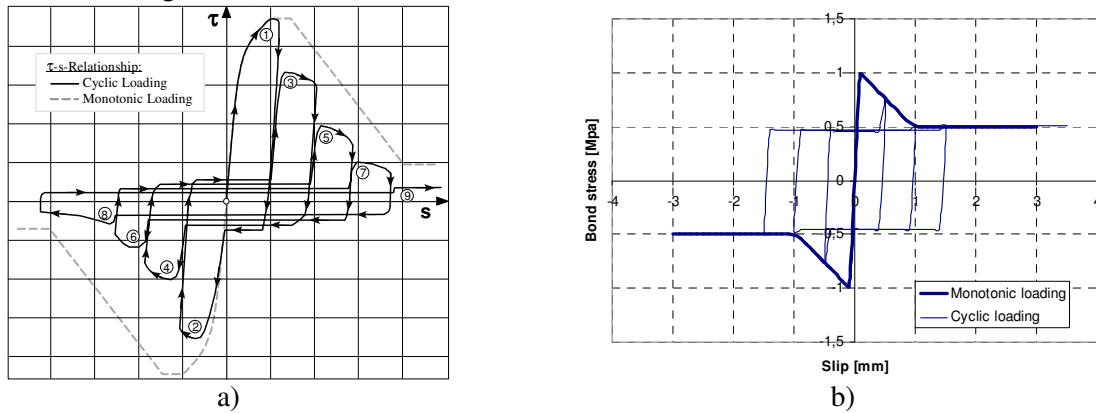

Figure 5. Bond-slip cyclic relationship: a) for deformed bars (Eligehausen et al. 1983); b) for smooth bars.

3.3 Modelling of the 180° hooks

Preliminary numerical studies carried out as part of this investigation, highlighted the difficulty to model the hook ended bars using 1D finite elements. The possibility to model these hooks with 3D solid elements was discarded due to the excessive computation effort required. Therefore, the discrete bond model implemented in MASA was calibrated to reproduce the stress-displacement behaviour of the hook as measured from the experiments. The calibration was performed using the test results of Fabbrocino et al. (2002). They used hooked bars with diameter d = 12 mm. In Figure 6a the concept for modelling of the smooth reinforcement with hooked ends is shown schematically. The discrete bond-slip of the hook was assumed to be linear elastic ($\tau_m + \tau_f \rightarrow \infty$). The stiffness of the hook was calibrated by detailed 3D FE analysis (Figure 6b).
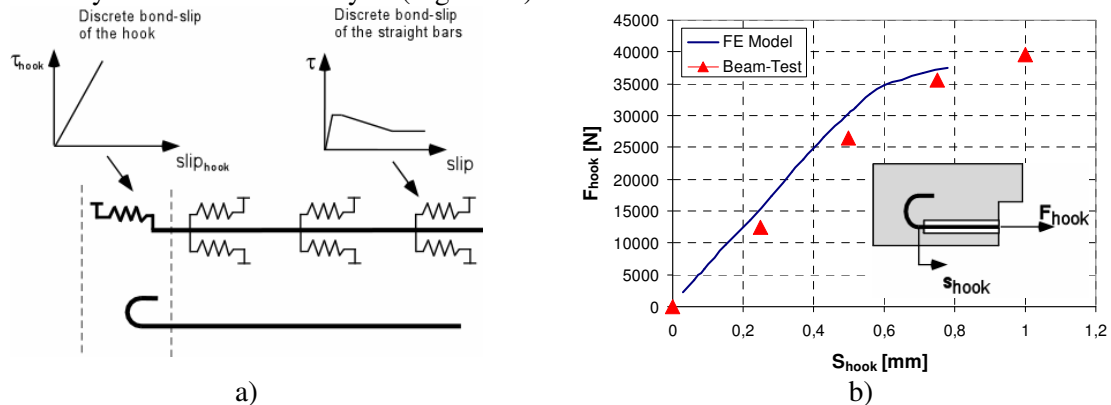

Figure 6 Modelling of the hooked reinforcement: a) basic concept; b) calibration using the beam tests of Fabbrocino et al. (2002).

3.4 Spatial discretization and material properties

The loading configuration is shown schematically in Figure 7a. In the analysis, two different finite element models were used. For monotonic loading, a relatively fine discretization was employed (Figure 7b). On the other hand, in order to save computation time for this phase of the project, cyclic analyses were carried out using a relatively coarse discretization (Figure 7c). In the actual analysis, the vertical symmetry of the specimens required that only one-half of the specimen be modelled. The concrete was discretised by eight-node solid finite elements. Reinforcement was represented by 1D truss elements. The connection between all longitudinal reinforcement and the concrete was modelled

4

by discrete bond. For the transverse reinforcement, a rigid connection between reinforcement and concrete was assumed. The basic material properties used in the FE analysis are summarized in Table 1 and Table 2.

The concrete elements in the vicinity of the supports were taken to be linear elastic to prevent local failure of concrete.

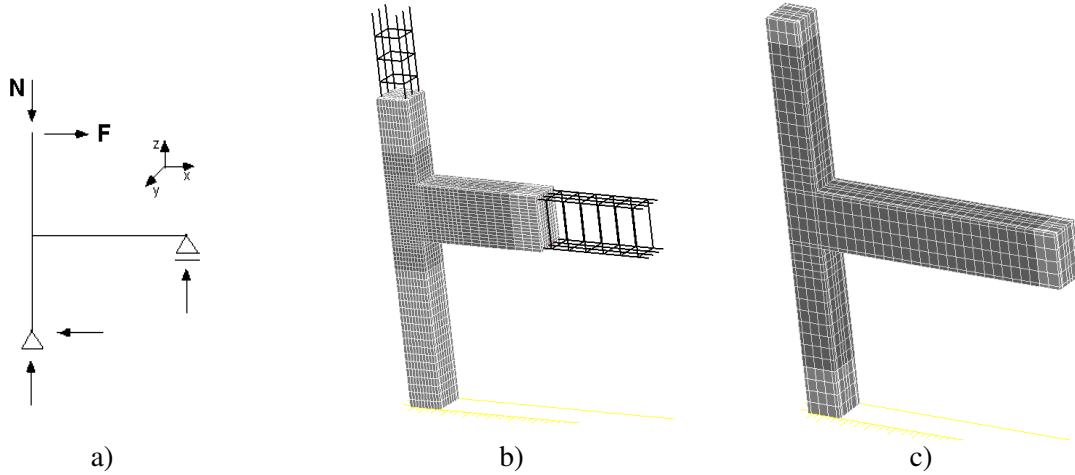| a) | b) | c) |

Figure 7. Model of test specimen: a) static system; b) fine 3D FE mesh used for monotonic loading; c) coarse 3D FE mesh used for cyclic loading

Table 1 Material parameters used in the numerical simulation.

Basic material properties				
Concrete	Cylinder compression strength 23.9 MPa		Tensile strength 1.80 MPa	
	Young's modulus 28800 N/mm^2	Poisson's ratio 0.18	Fracture energy 0.062 N/mm	
Steel	Yielding strength	Ultimate strength	Young's modulus	Hardening modulus
Ø 4	375 MPa	403 MPa	210000 MPa	2000 MPa
Ø 8	385 MPa	451 MPa	210000 MPa	2000 MPa
Ø 12	345 MPa	458 MPa	210000 MPa	2000 MPa

Table 2 Bond parameters used in the numerical simulation (parameters described in Figure 4).

Basic discrete bond properties for straight bars				
Monotonic and cyclic loading	$k_{secant} =$	80 N/m	$s_2 =$	0.1 mm
	$k_1 =$	100 N/m	$s_3 =$	1.0 mm
	$k_2 =$	10 N/m	$\tau_m =$	0.5 MPa
	$k_{unload} =$	100 N/m	$\tau_f =$	0.5 MPa
Basic discrete bond properties for 180° hook				
Monotonic loading	$k_{secant} =$	50 N/m	$s_2 =$	10 mm
	$k_1 =$	80 N/m	$s_3 =$	20 mm
	$k_2 =$	10 N/m	$\tau_m =$	500 MPa
	$k_{unload} =$	80 N/m	$\tau_f =$	1 MPa
Cyclic loading	$k_{sec} =$	80 N/m	$s_2 =$	10 mm
	$k_1 =$	100 N/m	$s_3 =$	20 mm
	$k_2 =$	10 N/m	$\tau_m =$	500 MPa
	$k_{unload} =$	100 N/m	$\tau_f =$	1 MPa

4 RESULTS AND COMPARISON WITH EXPERIMENTAL DATA

4.1 Monotonic loading

Figure 8 compares the lateral force versus top drift (L-D) curves for monotonic loading of the fine and coarse models with the envelope curve from the cyclic experiments. It can be seen that the numerical results agree reasonably well with the experimental results. The coarse model, however, slightly overestimated the peak resistance and exhibited slightly more brittle response. For both models the failure mode was diagonal shear failure of the joint.
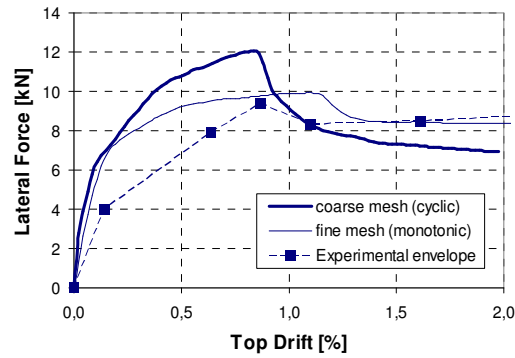
Figure 8. Comparison of the model response for the coarse and fine meshes with experimental results

Figure 9 shows the predicted failure mode for the fine finite element mesh. The system was characterized by flexural behaviour up to approximately 1,1% top drift (Figure 9a), at which point shear cracking in the joint became evident and the flexural cracks stopped growing. The joint shear crack, which ultimately caused the model to fail, was similar to the shear cracks observed in the experiments (Figure 9d). Unfortunately, a direct comparison of the sequence of cracking (flexural to shear) was not possible since monotonic loading of the test specimens was not performed.
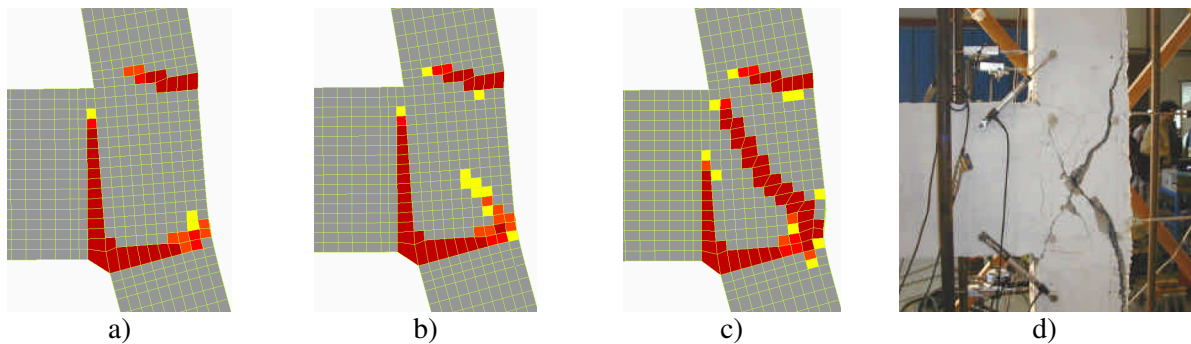

| a) | b) | c) | d) |

Figure 9. Cracking under monotonic load at different top drift levels: a) 1.09%; b) 1.16%; c) 1.50%; d) cracking in the test specimen after cyclic loading

The finite element model for monotonic loading (fine mesh) was also used to investigate: 1) the influence of the bond strength (Figure 10) and 2) the influence of the normal column force (Figure 10b). All parametric studies for monotonic loading were conducted using the basic material and bond properties (see Table 1 and Table 2).

Figure 10 shows the influence of the ultimate bond strength ($\tau_m + \tau_f$) on the response of the joint. It can be seen that with higher bond strength the resistance is higher and the failure more brittle. Figure 10 b) shows the influence of the axial column force on the lateral force versus top drift curve. It can be seen that with higher compressive force the joint shear (thus overall subassembly) resistance increases.
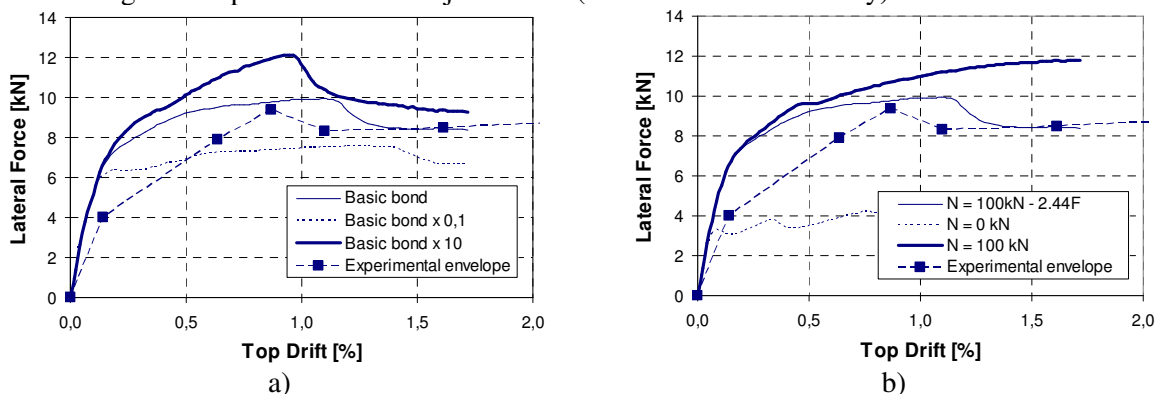

| a) | b) |

Figure 10. Comparison of numerical and experimental results for monotonic loading: a) effect of variation of the bond strength ($\tau_m + \tau_f$); b) effect of variation of axial force on the column

6

4.2 **Cyclic loading**

In the cyclic analyses the joint was loaded as explained in Section 2 (refer to Figure 2). Figure 11 shows the lateral force-lateral displacement (L-D) curve obtained from the experiment for the exterior joint T1. It is interesting to observe that although the diagonal shear cracking was initiated after a top drift of 0.86% the resistance of the system in the following loading cycles was not significantly decreased. The reason is probably due to the fact that the shear crack was not fully developed before reversed loading was applied. Moreover, due to the damage introduced through cyclic loading, the bending stiffness of the beam is significantly reduced and the force in the upper and lower reinforcement bars decreases with an increased number of loading cycles, thus limiting the nominal shear demand in the joint.
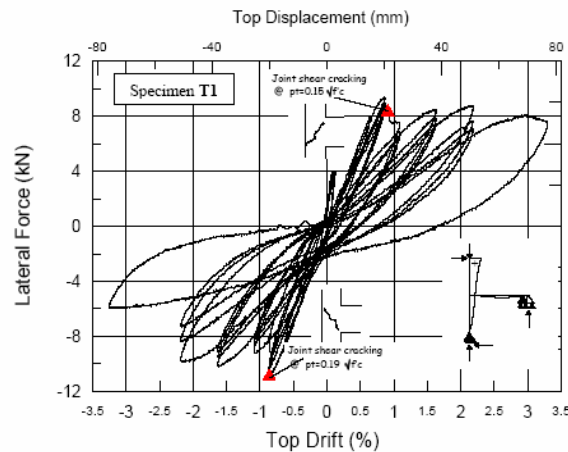

Figure 11. Experimental hysteresis loops for specimen T1 (Pampanin et al. 2002)

Figure 12 shows cracking in the joint under cyclic loading. The results in Figure 12a) were obtained using the basic material and bond properties in Table 1 and Table 2. In the model, bending cracks first formed in the beam (crack no. 1). Subsequently, cracks formed in the column (cracks no. 2 & 3). Finally, shear cracks formed in the joint (crack no. 4), which led to degradation of the resistance during subsequent cycles. The same cracking sequence was observed in comparable experimental tests performed by Braga et al. (2001) (Figure 12b). Note that crack no. 1 is not at the same location as in the case of monotonic loading (compare Figure 12a) with Figure 9a), i.e. it has moved away from the column. A possible reason for the move could be that the cyclic loading damaged the bond between the concrete and the reinforcement and consequently more bond length for transfer of force was needed. This must be confirmed, however, using a finer mesh under cyclic loading.

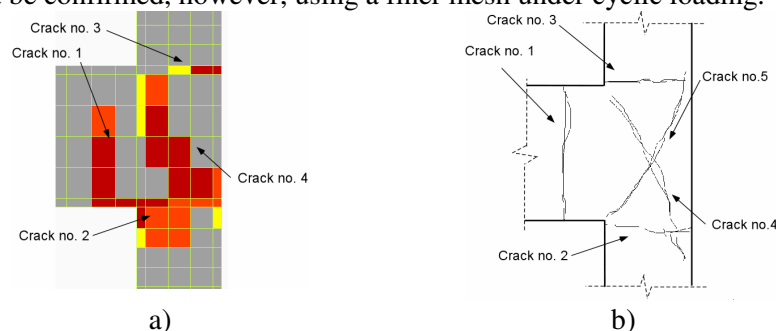a)   b)

Figure 12. Comparison of cracking during cycling: a) numerical model; b) experimental results from Braga et al. (2001)

The calculated L-D curve for the basic model is plotted in Figure 13. The degradation of the force in the model is stronger than that in the experiment (compare Figure 13 with Figure 11). This is probably due to the local bending resistance of reinforcement bars, which was not accounted for in the basic FE analysis. Recall that in the analysis of the basic model, the reinforcement was modelled by truss elements with no bending stiffness. Another possible cause of the severe degradation of force in the FE model could be that the finite element discretization was too coarse in the cyclic analysis.
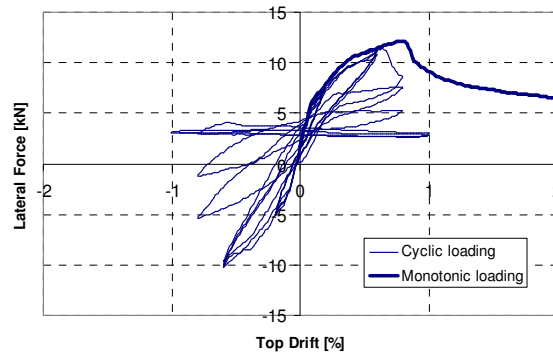
Figure 13. Numerical hysteresis loops for model calculated with basic material and bond properties

To better understand the behaviour of joints under cyclic loading, additional parametric numerical studies were carried out with particular attention on the influence of: 1) the degradation of bond properties due to cyclic loading, 2) the stiffness of the hooks, 3) the bending stiffness of reinforcement bars and 4) the bond strength of the longitudinal bars. In these calculations, one parameter was varied at a time, while maintaining the same configuration adopted in the basic cyclic analysis.

Figure 14b) was generated using a model in which the degradation of the bond resistance under cyclic loading was based on that used for deformed bars. This led to a smaller reduction of joint resistance during cycling when compared to the case where degradation rules for smooth bars were used (compare Figure 14b) with Figure 13). Failure in this case was due to formation of plastic hinges in the column (Figure 14a).
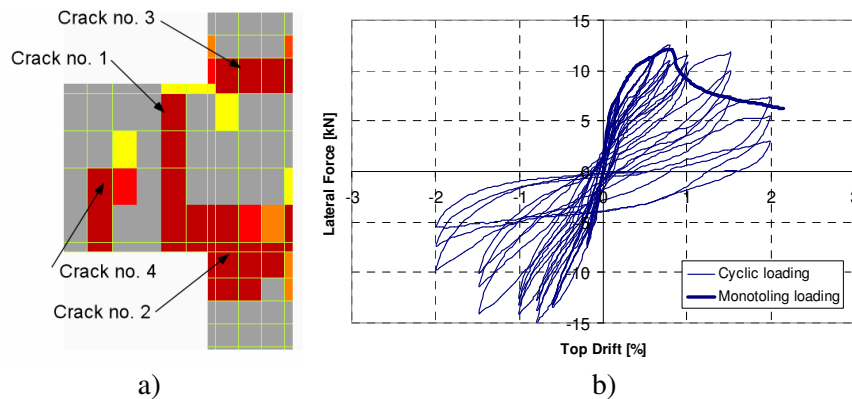

a)   b)

Figure 14. a) Failure due to formation of plastic hinge in the column; b) hysteresis loops obtained with bond degradation model typical of deformed bars

The same tendency was observed for the cases where the stiffness of the hooks was reduced (Figure 15a) or the bond strength was decreased (Figure 15b). Furthermore, if bending stiffness of the reinforcement was taken into account, the hysteresis response was closer to the experimentally measured results. Figure 15c shows that by accounting for the bending stiffness of the reinforcement, compared to the basic model, the results show more ductile behaviour with larger displacement before failure.

Figure 14b) and Figure 15a) to Figure 15c) indicate that, regardless of the varied parameter, the monotonic loading always led to shear failure. Furthermore, the overall resistance was usually lower for monotonic loading than for cyclic loading. The reason is possibly due to the redistribution of the stiffness, and therefore internal stresses, as a consequence of cyclic loading. More detailed studies are needed to understand this behaviour.
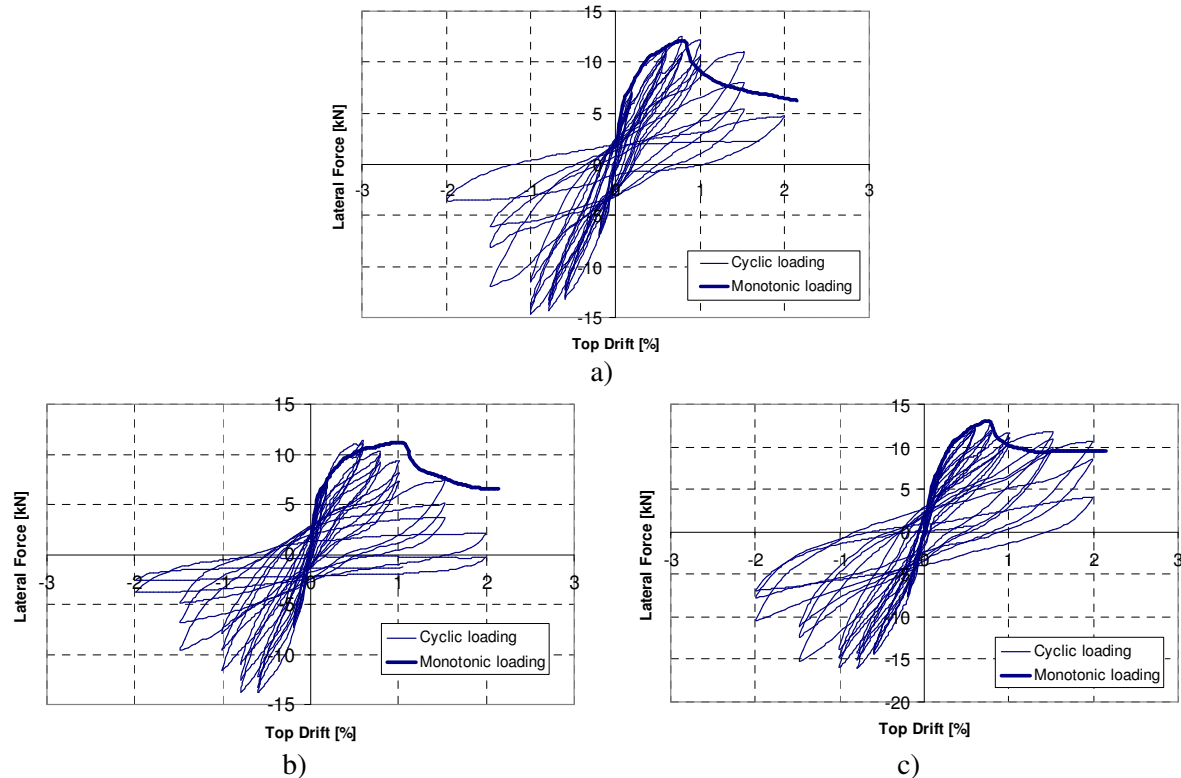
Figure 15. Hysteresis loops for various models: a) model without bond degradation and with lower hook stiffness (x0,25); b) model without bond degradation and with reduced bond strength ($\tau_m + \tau_f = 0.25 + 0.25$ MPa); c) model taking account of the bending stiffness of reinforcement.

5 CONCLUSIONS

The following conclusions can be derived based on the results of the experimental and numerical studies:

1) The numerical analysis of monotonic loading shows clear diagonal shear cracks. The envelope of cyclic loading from experiments agrees reasonably well with the results of the monotonic analysis. The parametric study confirmed that rigid bond between the reinforcement and the concrete and an increased level of axial force in the column increase the resistance of the overall subassembly.

2) The experimental results showed progressive stiffness and overall strength degradation due to the increasing number of cycles and level of imposed lateral displacement. It is interesting to observe, however, that in spite of the extensive diagonal cracks that occurred in this beam-column specimen, the strength degradation of the T1 specimen due to subsequent cyclic loading was less critical than that predicted by the numerical model (and expected from a pure shear failure mechanism) as described in the following point.

3) Cyclic analysis of the basic model showed diagonal shear cracking with a subsequent strong reduction of strength and stiffness. The crack development was similar to that observed during the experimental tests; however, the reduction of strength and stiffness was higher than in the experiments. The reason is probably due to the fact that the local bending stiffness of reinforcement, which was not accounted for in the basic cyclic analysis, contributes to the resistance and prevents sudden failure typical for shear. Another reason may be that the finite element mesh used for the cyclic analysis was too coarse.

4) The parameter study showed that the bond resistance, the hook stiffness and local bending stiffness of reinforcement significantly influenced the cyclic response. With decreased bond strength and decreased hook capacity, there was less reduction of the strength and stiffness

with an increasing number of loading cycles. The damage and failure mode also changed from shear to flexural type, with the formation of a plastic hinge in the column. The same tendency was observed when the local bending stiffness of the reinforcement was taken into account.

5) It is interesting to observe that for monotonic loading using the coarse mesh, i.e. the mesh used for cyclic loading, failure was always due to diagonal shear cracking. The relatively ductile response of these models under cyclic loading indicates that the distribution of forces in the beam-column connection was strongly influenced by the load cycling.

Further numerical and experimental investigations are needed to clarify a number of open questions. Moreover, in the next phase of the project the behaviour of the connection with strengthening measures using post-installed fasteners on the subassemblies will be investigated.

REFERENCES:

Braga F, De Carlo G., Gigliotti R., Laterza M., Nigro. D., 2001. Meccanismi di risposta di nodi trave-pilastro in c.a. di strutture non antisismiche. *X Congresso Nazionale "L'ingegneria sismica in Italia", Potenza-Matera 2001.*

Eligehausen, R., Popov, E.P., Bertero, V.V., 1983. Local bond-stress relationships of deformed bars under generalised excitation, *UCB/EERC 83, 23.*

Fabbrocino G., Verderame G.M., Manfredi G. and Cosenza E., 2002. Experimental behaviour of smooth bars anchorages in existing r.c. Buildings. *First fib congress 2002 "Concrete structures in the 21st Century", paper w-463.*

Lettow, S. 2006. Ein Verbundelement für nichtlineare Finite Elemente Analysen - Anwendung auf Übergreifungsstöße. *Dissertation, Institut für Werkstoffe im Bauwesen, Universität Stuttgart, 2006.*

Ožbolt, J., Li, Y., and Kožar, I., 2001. Microplane model for concrete with relaxed kinematic constraint. *International Journal of Solid and Structures.*

Ožbolt, J., Lettow, S.and Kožar, I., 2002. Discrete Bond Element for 3D Finite Element Analysis of Reinforced Concrete Structures.

Pampanin, S., Calvi, G.M. and Moratti, M., 2002. Seismic Behaviour of R.C. Beam-Column Joints Designed for Gravity Only, *Proceedings of the 12th European Conference on Earthquake Engineering*, paper n.726, London, September.

Seismic Response of reinforced Concrete Buildings Designed for Gravity Loads. Part I: Experimental Test on Beam-Column Subassemblies. *Submitted to ASCE Journal of Structural Engineering.*

Park, R., 2002. A summary of results of Simulated Load Tests on Reinforced Concrete Beam-Column Joints, Beams and Columns with Substandard Reinforcing Details. *Journal of Earthquake Engineering, Vol. 6, No. 2, 1-27.*